Copper Mediates Dityrosine Cross-Linking of Alzheimer's Amyloid-β[†]

Craig S. Atwood,*[,‡,§] George Perry,[‡] Hong Zeng,[‡] Yoji Kato,[||] Walton D. Jones,[‡] Ke-Qing Ling,[⊥] Xudong Huang,[@,#] Robert D. Moir,[#] Dandan Wang,[‡] Lawrence M. Sayre,[⊥] Mark A. Smith,[‡] Shu G. Chen,[‡] and Ashley I. Bush[@,#,○]

Institute of Pathology, Case Western Reserve University, Cleveland, Ohio 44106, Centre for Aging and Alzheimer's Disease, School of Biomedical & Sports Science, Edith Cowan University, Joondalup, WA 6027, Australia, Department of Chemistry, Case Western Reserve University, Cleveland, Ohio 44106, School of Humanities for Environmental Policy and Technology, Himeji Institute of Technology, Himeji, Hyogo 670-0092, Japan, and Laboratory for Oxidation Biology, Department of Psychiatry, and Genetics and Aging Unit, Harvard Medical School, Massachusetts General Hospital, Charlestown, Massachusetts 02129

Received October 20, 2003; Revised Manuscript Received November 6, 2003

ABSTRACT: We have previously reported that amyloid Aβ, the major component of senile plaques in Alzheimer's disease (AD), binds Cu with high affinity via histidine and tyrosine residues [Atwood, C. S., et al. (1998) *J. Biol. Chem. 273*, 12817−12826; Atwood, C. S., et al. (2000) *J. Neurochem. 75*, 1219−1233] and produces H_2O_2 by catalyzing the reduction of Cu(II) or Fe(III) [Huang, X., et al. (1999) *Biochemistry 38*, 7609−7616; Huang, X., et al. (1999) *J. Biol. Chem. 274*, 37111−37116]. Incubation with Cu induces the SDS-resistant oligomerization of Aβ [Atwood, C. S., et al. (2000) *J. Neurochem. 75*, 1219−1233], a feature characteristic of neurotoxic soluble Aβ extracted from the AD brain. Since residues coordinating Cu are most vulnerable to oxidation, we investigated whether modifications of these residues were responsible for Aβ cross-linking. SDS-resistant oligomerization of Aβ caused by incubation with Cu was found to induce a fluorescence signal characteristic of tyrosine cross-linking. Using ESI-MS and a dityrosine specific antibody, we confirmed that Cu(II) (at concentrations lower than that associated with amyloid plaques) induces the generation of dityrosine-cross-linked, SDS-resistant oligomers of human, but not rat, Aβ peptides. The addition of H_2O_2 strongly promoted Cu-induced dityrosine cross-linking of Aβ1−28, Aβ1−40, and Aβ1−42, suggesting that the oxidative coupling is initiated by interaction of H_2O_2 with a Cu(II) tyrosinate. The dityrosine modification is significant since it is highly resistant to proteolysis and is known to play a role in increasing structural strength. Given the elevated concentration of Cu in senile plaques, our results suggest that Cu interactions with Aβ could be responsible for causing the covalent cross-linking of Aβ in these structures.

The amyloid lesions of AD are primarily composed of Aβ (*5*, *6*), a 39−43-amino acid protein that is a normally soluble protein found in biological fluids (*7*−*9*). Although Aβ from biological fluids migrates as an ∼4 kDa monomer on SDS−PAGE (*9*), Aβ extracted from the AD-affected post mortem brain specimens migrates on sodium dodecyl sulfate−polyacrylamide gel electrophoresis (SDS−PAGE) as SDS-, urea-, and formic acid-resistant oligomers (*6*, *10*, *11*). Synthetic Aβ1−40 and Aβ1−42 normally migrate as monomers on SDS−PAGE (*12*) but form higher-molecular mass species upon incubation (*12*, *13*), a process that is accelerated by added Cu(II) (*2*) and exposure to oxidative systems (*14*, *15*). The chemical nature of the modifications and the specific neurochemical mechanism(s) responsible for these oligomerized Aβ species are unknown.

We have been studying Cu, Zn, and Fe as abundant neurochemicals that interact with Aβ (*1*, *16*−*18*). We have found that Aβ simultaneously binds equal amounts of Cu(II) and Zn(II) in PBS at pH 7.4 (∼1.8 atoms each), while the highest affinity of Cu(II) for Aβ1−42 (log K_{app} = 17.2) is much greater than that of Cu(II) for Aβ1−40 (log K_{app} = 10.3) (*2*). The levels of these metals are all markedly higher within AD neuropil than within age-matched control neuropil, and are even further concentrated within plaque deposits (*19*). Using Raman microscopy, we recently demonstrated that senile core plaques isolated from the AD brain are predominantly composed of Aβ protein bound to Cu(II) and Zn(II) via histidine residues (*20*). These results help explain the enrichment of these metals in plaque amyloids.

We have previously reported that Aβ reduces Cu(II) and Fe(III) to Cu(I) and Fe(II), respectively, with the consequent generation of H_2O_2 from O_2 (*3*, *4*). We further reported that incubation of Aβ with Cu oxidation systems damages

[†] This work was supported by funds from the National Institutes of Health through a pilot award from the University Hospitals of Cleveland/Case Western Reserve University Alzheimer's Disease Research Center (Grant P50AG08012 to C.S.A.) and by NIH Grants RO1 AG19356 (to C.S.A.) and RO1 AG14249 to (M.A.S.).

* To whom correspondence should be addressed. Present address: University of Wisconsin Medical School, William S. Middleton Memorial VA Hospital (GRECC 11G), 2500 Overlook Terrace, Madison, WI 53705. Phone: (608) 256-1901, ext. 11664. Fax: (608) 280-7291. E-mail: csa@medicine.wisc.edu.

[‡] Institute of Pathology, Case Western Reserve University.

[§] Edith Cowan University.

[||] Himeji Institute of Technology.

[⊥] Department of Chemistry, Case Western Reserve University.

[@] Laboratory for Oxidation Biology, Department of Psychiatry, Harvard Medical School, Massachusetts General Hospital.

[#] Genetics and Aging Unit, Harvard Medical School, Massachusetts General Hospital.

[○] Mental Health Research Institute of Victoria, and Department of Pathology, University of Melbourne, Parkville 3050, Victoria, Australia.

10.1021/bi0358824 CCC: $27.50
Published on Web 12/20/2003

tyrosine and histidine residues (*21*), which are known to coordinate Cu in Aβ (*1*, *22*). We therefore hypothesized that in the elevated Cu ($\sim$400 μM; *19*, *20*) environment of the senile plaque, there may be an increased likelihood of oxidative damage of amino acids that coordinate Cu, mediated by H_2O_2 perhaps in part generated by the redox cycling of the same Cu. We report here that Aβ is tyrosine cross-linked by Cu at concentrations lower than those detected in senile plaques *in vivo* (*19*), resulting in the generation of oligomeric Aβ species.

EXPERIMENTAL PROCEDURES

Reagents and Aβ Peptide Preparation. *N*,*N*′-Diacetyldi-L-tyrosine (DADT)[1] has been prepared on an analytical high performance-liquid chromtography (HPLC) scale by direct photochemical (*23*) or HRP- and H_2O_2-mediated (*24*) oxidative coupling of *N*-acetyl-L-tyrosine (AT), but production on a preparative scale was achieved here according to modifications of established procedures. Briefly, *N*-acetyl-3,5-diiodo-L-tyrosine (ADIT) was first prepared either by iodination of AT with iodosuccinimide or by acetylation of 3,5-diiodo-L-tyrosine. Then ADIT was oxidatively coupled using HRP and H_2O_2, providing a mixture of the desired biphenol and an undesired spirocyclohexadienone side product which is reduced *in situ* to the biphenol with $NaHSO_3$ (*25*). In our hands, the 8 mmol scale reaction gave optimal yields using 25% rather than 10% acetonitrile in pH 6 aqueous phosphate buffer. The resulting 3,3′-diiodo-*N*,*N*′-diacetyldi-L-tyrosine was hydrogenated to DADT in 50% methanolic acetic acid, which gave much better yields than the aqueous methanolic HCl used for hydrogenation of the di-CBZ compound (*26*). Conversion of DADT to di-L-tyrosine (DT) was accomplished by heating a solution of DADT in a 1:1 mixture of tetrahydrofuran and concentrated HCl at reflux for 4 h under argon. Complete evaporation of the solvent yielded the di-HCl salt of DT.

Human Aβ1−40 and Aβ1−42 were synthesized and purified by HPLC and characterized by amino acid analysis and mass spectroscopy by the W. M. Keck Foundation Biotechnology Resource Laboratory (Yale University, New Haven, CT). Both peptides were identified as a single peak upon HPLC and exhibited no chemical modification. Rat Aβ1−40 and human Aβ1−28 were purchased from AnaSpec (San Jose, CA). The sequence of each peptide is shown below.

	1 10 20 30 40
Human Aß1-40	DAEFRHDSGYEVHHQKLVFFAEDVGSNKGAIIGLMVGGVV
Human Aß1-42	DAEFRHDSGYEVHHQKLVFFAEDVGSNKGAIIGLMVGGVV**IA**
Rat Aß1-40	DAEF**G**HDSG**F**EV**R**HQKLVFFAEDVGSNKGAIIGLMVGGVV
Human Aß1-28	DAEFRHDSGYEVHHQKLVFFAEDVGSNK

Synthetic Aβ peptide solutions were dissolved in doubly deionized water at a concentration of 0.5−1.0 mg/mL, sonicated for 3 min, and then centrifuged for 20 min at 10000*g*, and the supernatant (stock Aβ) was used on the day of the experiment. The concentrations of stock Aβ peptides were determined by the spectrophotometric absorbance at 214 nm or by a Micro BCA protein assay (Pierce, Rockford, IL) as previously described (*1*). Prior to use, all buffers and stock solutions of metal ions were filtered though a 0.22 μm filter (Gelan Sciences, Ann Arbor, MI) to remove particulate matter. Metal ions were used as either the chloride salt or the copper−glycine complex (1:2 molar ratio). All other reagents were analytical grade or purer.

Model Studies on the Cu(II)-Mediated Oxidative Coupling of N-Acetyl-L-tyrosine (AT). Various combinations of AT (0.5 mM), $CuSO_4$ or $CuCl_2$ (0−0.125 mM), ligand (imidazole or ethylenediamine, up to 0.5 mM), and H_2O_2 (up to 10 mM) were incubated at 25 °C for 48 h in 0.1 M phosphate buffer (pH 7.4). In some reaction mixtures, an additive (mannitol or ethylene glycol as $OH^{\bullet}$ scavengers) or chelator [EDTA or diethylenetriaminepentaacetic acid (DTPA)] was also present. Consumption of AT was assessed by monitoring the decreased absorption at 275 nm, and the yield of DADT was estimated by the emission intensity at 410 nm with excitation at 320 nm, relative to a standard curve constructed with authentic DADT.

Preparation and Characterization of Aβ Exposed to Redox Stressors. Aβ stock solutions were diluted to 5−10 μM in PBS [50 mM phosphate and 150 mM NaCl (pH 7.4)] and incubated with combinations of Cu(II), Fe(III), and H_2O_2 for 0−5 days at 37 °C. Aβ solutions were analyzed for the presence of fluorescent compounds using an SLM-Aminco fluorimeter (Spectronic Instruments, Milton Roy Co.). DT, trityrosine, and pulcherosine have characteristic emission spectra (λ_{ex} = 300 nm, λ_{em} = 350−500 nm) that are quite distinct from those of tyrosine and tryptophan, which do not fluoresce at these wavelengths. There was a linear increase in fluorescence with increasing dityrosine concentration between 0 and 5 μM.

Immunoblot Analysis. Aliquots of each reaction mixture (200 ng of peptide) were collected into 15−30 μL of sample buffer (containing 4% SDS and 5% β-mercaptoethanol) and heated to 95 °C (5 min). Samples were loaded and run on SDS−PAGE (Tricine gels, from 10 to 20%; Novex, San Diego, CA), transferred to PVDF membranes (Bio-Rad Laboratories, Hercules, CA), fixed with glutaraldehyde (1%, v/v), blocked with milk (10%, w/v), and then probed with a monoclonal antibody against Aβ (4G8; Senetek, Maryland Heights, MI) or dityrosine (G6 or 1C3) (*27*) overnight at 4 °C. The blot was then incubated with an anti-mouse HRP conjugate (Pierce) for 2 h at room temperature, and developed with ECL reagent (1 min; Amersham, Little Chalfont, England) or Supersignal Ultra (5 min; Pierce) by following the manufacturer's instructions. The chemiluminescent signal was captured on autoradiographs (Kodak). Molecular size markers are from Amersham (Arlington Heights, IL).

For dot blots, 5 μg of sample was loaded onto a methanol-wetted PVDF membrane (Bio-Rad Laboratories) prior to fixing and processed as described above. Preabsorption of antibodies G6 and 1C3 was performed with DADT.

Analysis of Dityrosine by HPLC and Electrospray Ionization Mass Spectrometry (ESI-MS). Aβ stock solutions were diluted to 10 μM in PBS (pH 7.4) and incubated with Cu(II) (50 μM) with or without H_2O_2 (250 μM) for 3 days at 37 °C. The samples (200 μL) were subjected to acid hydrolysis in the presence of 6 N HCl under nitrogen at 110 °C for 24

[1] Abbreviations: ADIT, *N*-acetyl-3,5-diiodo-L-tyrosine; AT, *N*-acetyl-L-tyrosine; DADT, *N*,*N*′-diacetyldi-L-tyrosine; PBS, phosphate-buffered saline; ROS, reactive oxygen species; SDS−PAGE, sodium dodecyl sulfate−polyacrylamide gel electrophoresis.

h. The hydrolysates were dried by vacuum, and were formyl derivatized in the presence of 20 μL of 0.1% formic acid for 2 h at 40 °C to enable the analysis of dityrosine by reverse phase HPLC on a C18 column (see below). The chemically synthesized dityrosine (0.6 μg), derivatized under identical conditions, was used as a standard. Samples were separated by HPLC on a microbore column (C18aq, 5 μm, 100 Å, 1.0 mm × 150 mm, Michrom BioResources) at 50 μL/min with a gradient of 5 to 20% acetonitrile containing 0.1% formic acid for 30 min. The eluates were monitored by the UV absorbance at 280 nm, and were analyzed by on-line ESI-MS. ESI-MS was performed with an ion trap LCQ mass spectrometer (LCQ^{DUO}, Finnigan). The mass spectrometer was equipped with an ESI needle with an ion spray voltage set at 3000 V and with nitrogen as the sheath gas. The capillary temperature and sheath gas pressure were set at 160 °C and 80 psi, respectively. An MS scan (*m*/*z* 150−2000) was performed in the positive ion acquisition mode to detect intact molecular ions. The formyl derivative of dityrosine (*N*,*N*′,*O*-triformyldityrosine) was detected as $[M + H]^+$ at *m*/*z* 445. The identification of *N*,*N*′,*O*-triformyldityrosine was further confirmed by collision-induced dissociation using the tandem MS/MS scan.

RESULTS

Copper Induces the Formation of SDS-Resistant Aβ Species. Aβ1−40 represents the most commonly produced form of Aβ (*28*). Immunoblot analysis of Aβ1−40 in PBS (pH 7.4), incubated for 0 or 3 days, indicated the presence of a small amount of dimeric (8.6 kDa) Aβ. The effects of metal ion oxidation were tested by incubating Aβ1−40 with or without Cu(II) (25 μM). Immunoblot analysis of samples incubated with Cu(II) revealed an increase in higher-molecular mass Aβ species within 24 h (Figure 1; *2*), and levels continued to increase with time (data not shown). Apparent dimeric, trimeric, and tetrameric species had relative molecular masses (M_r) of approximately 8.6, 13.0, and 17 kDa, respectively.

Aβ1−42 is enriched in senile plaques (*6*, *29*−*31*). We next compared the ability of Cu(II) to modify Aβ1−42. Unlike Aβ1−40 where Cu(II) induces the formation of a 8.6 kDa species first, Aβ1−42 forms a species that migrates with an apparent molecular mass of 13.0 kDa in the presence of Cu(II) (*2*). Longer incubations (>3 days) resulted in the appearance of an 8.6 kDa band, and apparent higher-molecular mass polymeric species (>13 kDa; Figure 1A). Since >90% of the Aβ1−42 present is instantaneously aggregated when it is incubated with Cu(II) (*2*), the slow modification of Aβ that causes SDS resistance most likely occurs while the peptide is in an aggregated state. Incubation with similar concentrations of Zn(II) or Fe(III) failed to induce oligomerized Aβ species (C. S. Atwood et al., not shown). Thus, the oligomers formed in the absence of added Cu may result from the slow oxidation of Aβ during or after synthesis due to trace Cu impurities which we have found are present in the purification systems or buffers (*2*, *3*; see below).

Cu(I), formed by the reduction of Cu(II) stimulated by binding to Aβ, generates H_2O_2 by transferring an electron to O_2 (*3*). To determine whether either the specific reduction of metal ions or the specific production of reactive oxygen species (ROS) was required for the generation of high-molecular mass Aβ species, we investigated whether the presence or absence of H_2O_2 could modulate the Cu-induced oligomerization of Aβ (Figure 1A). The level of oligomerization of Aβ1−40/42 in the presence of H_2O_2 alone was equivalent to background levels (data not shown). However, the addition of H_2O_2 in the presence of Cu(II) induced a marked increase in the level of higher-molecular mass species for both peptides (Figure 1A; >18 kDa), accompanied by a decrease in the levels of monomeric Aβ. Two distinct higher-molecular mass species of Aβ were generated under these conditions. The levels of apparent dimeric (8.6 kDa) and trimeric (13 kDa) bands of Aβ, present otherwise at only low levels in the presence of Cu(II) alone, were increased with added H_2O_2, and an apparent tetrameric species (17 kDa) was now present as well. Under these harsher oxidative conditions [Cu(II) and H_2O_2], apparent higher-molecular mass Aβ species (>17 kDa) were now also observed (Figure 1A), perhaps recruiting intermediate 8.6−17 kDa species.

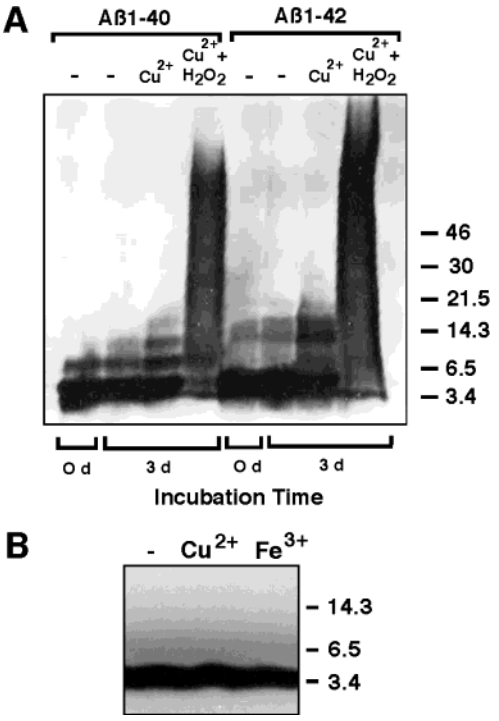

FIGURE 1: Copper-induced oligomerization of human, but not rat, Aβ peptides. (A) Human Aβ1−40 or Aβ1−42 (5 μM) was brought to 150 mM NaCl and 66 mM phosphate (pH 7.4) with or without Cu(II) (25 μM) and H_2O_2 (250 μM). (B) Rat Aβ1−40 was brought to 150 mM NaCl and 66 mM phosphate (pH 7.4) with or without Cu(II) or Fe(III) (25 μM). Samples were incubated at 37 °C for 1 day, and aliquots were analyzed by immunoblots (4G8 antibody). Results are representative of three experiments.

To test whether metal ions could induce similar SDS resistance of rat Aβ1−40, which contains three amino acid substitutions [Arg^5Gly, $Tyr^{10}Phe$, and $His^{13}Arg$ (*32*)], rat Aβ1−40 was incubated with Cu(II) and Fe(III) (Figure 1B). In contrast to the effects of Cu(II) upon human Aβ1−40 and Aβ1−42 (Figure 1A), neither metal ion induced modifications of rat Aβ after 3 days as detected by immunoblot analysis. The aggregation of rat Aβ1−40 by Cu(II) (*1*) and the reduction of Cu(II) by rat Aβ1−40 are both markedly attenuated compared to that of human Aβ (*3*). Taken together, these results suggest that the generation of higher-molecular mass Aβ species is dependent upon the specific

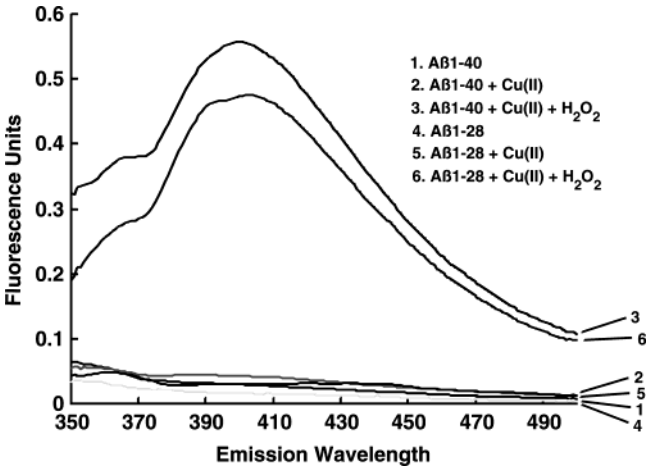

FIGURE 2: Aβ develops fluorescence following Cu-catalyzed oxidation. Aβ1−40 and Aβ1−28 (10 μM) were incubated in PBS (pH 7.4) with or without Cu(II) (25 μM) and H_2O_2 (250 μM) at 37 °C, and the fluorescent spectra (λ_{ex} = 300 nm, λ_{em} = 350−500 nm) of each sample were recorded after 1 day. Results are representative of three experiments.

Table 1: Cu-Catalyzed Oxidation of Rat Aβ Does Not Promote Fluorescence Indicative of Tyrosine Cross-Linking[a]

	no addition	with Cu(II)	with Cu(II) and H_2O_2
human Aβ1−40	0.052 ± 0.006	0.080 ± 0.005	0.844 ± 0.027
human Aβ1−42	0.062 ± 0.007	0.104 ± 0.013	0.506 ± 0.040
rat Aβ1−40	0.056 ± 0.006	0.048 ± 0.008	0.043 ± 0.011

[a] Human Aβ1−40, human Aβ1−42, and rat Aβ1−40 (10 μM) were incubated in PBS (pH 7.4) with or without Cu(II) (50 μM) and H_2O_2 (250 μM) at 37 °C, and the fluorescent spectra (λ_{ex} = 300 nm, λ_{em} = 400 nm) of each sample were recorded after 3 days. Results are means ± the standard deviation of the mean (n = 3).

binding of Cu(II) by human Aβ, and the subsequent action of H_2O_2 arising, in the *in vitro* experiments, from reduction of bound Cu(II) to Cu(I) and reduction of O_2 by the latter.

Cu-Induced SDS-Resistant Aβ Oligomers Are Tyrosine-Cross-Linked. Our data indicate that Aβ oligomerization is stimulated by the generation of ROS. Since rat Aβ1−40 peptide was resilient to polymerization in the presence of Cu (Figure 1B), it was likely that the Arg (position 5), Tyr (position 10), and His (position 13) residues were involved in Cu-induced cross-linking reactions of Aβ. Since oxidative attack can promote the formation of a tyrosyl radical and the formation of dityrosine, we tested whether the copper-induced oligomerization of Aβ was due to tyrosine cross-linking. To do this, we assessed samples containing Aβ with or without Cu and H_2O_2 for the characteristic fluorescence spectra of dityrosine. Analysis of Aβ1−40 (and Aβ1−28) incubated with Cu(II) for 1 day indicated an increase in the characteristic fluorescence for tyrosine cross-links, a signal that was markedly enhanced by addition of H_2O_2 (Figure 2). A similar fluorescence pattern was observed for Aβ1−42 incubated under similar conditions (Table 1). Fluorescent peaks also were detected when these samples were excited at 350 nm (λ_{ex}), suggestive of other conjugated cross-linked species (not shown). We are currently pursuing this observation.

Since rat Aβ did not form SDS-resistant oligomers, we tested rat Aβ1−40 for dityrosine fluorescence to confirm that Cu oxidation did not form dityrosine-like fluorescence

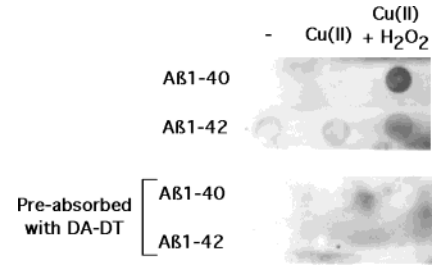

FIGURE 3: Cu(II) induces dityrosine immunoreactivity of Aβ. Synthetic Aβ1−40 and Aβ1−42 (5 μM in PBS, pH 7.4) were incubated (37 °C, 1 day) with or without Cu(II) (25 μM) and H_2O_2 (250 μM). Aliquots were analyzed by immunoblots (1C3 antibody) and immunosorbed with 10 μM purified *N*,*N*′-diacetyldi-L-tyrosine (DADT) (bottom panel).

in the absence of tyrosine. In contrast to human Aβ, no increase was observed in the fluorescence signal of rat Aβ1−40 after incubation with H_2O_2 and Cu (Table 1), suggesting that the fluorescent signal was specific for tyrosine oxidation products of Aβ.

To estimate the percentage of dityrosine generated in these reactions, we generated a dityrosine standard curve (y = 1.6574x + 0.0005, where y is in fluorescence units and x is the micromolar concentration of dityrosine; r^2 = 0.998; λ_{ex} = 300 nm, λ_{em} = 400 nm). The dityrosine content of Aβ1−40 increased by 0.25% after treatment with Cu(II) and 4.00% after treatment with Cu(II) and H_2O_2 for 3 days. The dityrosine content of Aβ1−28 increased by 0.16% after treatment with Cu(II) and 3.38% after treatment with Cu(II) and H_2O_2 for 3 days.

To verify that the fluorescent signal detected in these reactions was in fact due to tyrosine cross-linking of Aβ, we probed dot blots of these samples with the dityrosine specific antibody 1C3 (Figure 3). A signal for dityrosine was observed when Aβ1−40 or Aβ1−42 was incubated with both Cu(II) and H_2O_2. Unlike Aβ1−40, Aβ1−42 incubated with Cu for 1 day contained detectable dityrosine immunoreactivity, which was only faintly detectable in Aβ1−42 incubated alone. As noted above, the low background level of dityrosine observed with Aβ1−42 alone likely results from trace contamination of Cu in Aβ and buffers (*3*, *12*, *13*). The specificity of antibody binding to dityrosine was confirmed by preabsorbing the antibody with DADT (10 μM), and resulted in the loss of all dityrosine signals.

To analyze the cross-linking pattern of the oligomeric Aβ species that formed, we ran these samples on an immunoblot. This analysis revealed an increase in the level of dimeric Aβ species (M_r = 8.6 kDa) when Aβ1−40 was incubated with Cu(II), and increases in dimeric (M_r = 8.6 kDa), trimeric (M_r = 13 kDa), and higher oligomeric species when Aβ1−40 was incubated with Cu(II) and H_2O_2 [panels A (darker exposure) and B (lighter exposure) of Figure 4]. No tyrosine-cross-linked species were detected when Aβ1−40 was incubated alone. As for Aβ1−40, Cu(II)-dependent increases in the levels of oligomerized species also were observed for Aβ1−42 (Figure 4A). However, in addition to dimeric Aβ1−42 species, trimeric and tetrameric Aβ1−42 species (M_r = 13 and 17 kDa, respectively) also were detected (Figure 4A). H_2O_2 promoted the generation of higher-molecular mass species of Aβ1−42 in the presence of Cu(II); however, there was a decrease in signal intensity compared with Aβ1−40 incubated under similar conditions (see also Figure 3).

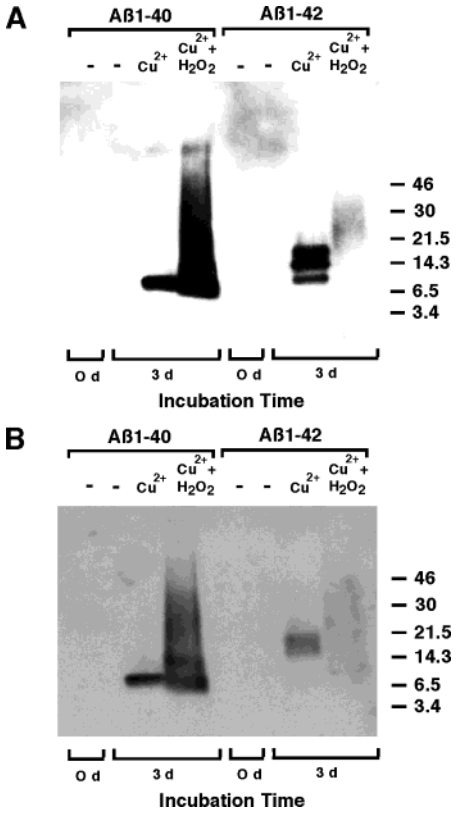

FIGURE 4: Cu(II) induces dityrosine cross-linked, SDS-resistant Aβ oligomerization. Aβ samples described in Figure 3 were analyzed with Western blots (1C3 antibody). (A) A darker exposure illustrates the oligomeric species of Aβ1−42 formed in the presence of Cu. Exposure of Aβ1−42 to Cu and H_2O_2 under these conditions sufficiently altered the peptide so that the level of antibody detection was significantly decreased compared with that of Aβ1−40. (B) A lighter exposure illustrates the formation of dimeric and trimeric Aβ1−40 species in the presence of Cu and H_2O_2. Results are representative of three experiments.

To confirm that Cu(II)-induced cross-linking of Aβ was via tyrosine residues, Aβ1−40 (10 μM) was incubated with Cu(II) (50 μM) in PBS (pH 7.4) for 3 days at 37 °C followed by acid hydrolysis and formyl derivatization. HPLC analysis of hydrolyzed and formylated samples indicated a peak at ~17 min, identical to that for the formyl-derivatized dityrosine standard (Figure 5A,B). This peak was subsequently identified using ESI-MS in both samples as *N*,*N*′,*O*-triformyldityrosine (Figure 5C,D) at *m*/*z* 444.8 ($[M + H]^+$). These results therefore indicate that Cu(II) induces the formation of dityrosine between Aβ molecules.

Mechanism of Dityrosine Formation. The mechanism of metal-mediated oxidative coupling of tyrosine to give DT was recently shown to be affected by H_2O_2 and Cu(II), with no dependence on the concentration of dissolved O_2 (*33*). These workers showed that whereas other metal-catalyzed oxidation systems that induce Fenton chemistry could transform tyrosine into oxygenated forms containing reactive carbonyl groups (presumably quinones), these systems were ineffective in producing dityrosine (*33*), apparently excluding $HO^\bullet$ as the effective oxidant in dityrosine formation.

Consistent with the published results, the Cu-mediated oxidative coupling of AT to give DADT was here confirmed to strictly require H_2O_2 in that the use of ascorbic acid and O_2 was ineffective whether a ligand (imidazole or ethylenediamine, to mimic peptide-bound Cu) was employed. The maximal absolute yield of DADT generated in 24 h at 25 °C was 1.5−2.0% under conditions where only 5−30% of the AT was consumed. Interestingly, in the presence of imidazole, the omission of Cu(II) from the incubations inhibited (by ~25%) but did not eliminate DADT formation. On the other hand, inclusion of as little as 1 μM DTPA in these cases completely eliminated DADT formation, suggesting that traces of transition metal present in the reagents are sufficient to mediate oxidative AT coupling, thus showing that the role of the metal is catalytic. Since this means that the factor limiting the yield of DADT was not conversion of the metal to inactive forms (assays also showed that the H_2O_2 was not consumed), we suspected that the reaction might just be slow. Indeed, the level of production of DADT was shown to increase steadily over 140 h at 25 °C (Figure 6), where the inclusion of ethylenediamine, and to a lesser extent imidazole, stimulated DADT formation relative to an environment with no added ligand, consistent with the improved redox activity of coordinated Cu. In these cases, the additional presence of ethylene glycol (15 mM) improved the yield in every case (Figure 6), apparently by suppressing the consumption of starting AT (data not shown) that is diverted to other oxidation products. Since ethylene glycol is known to quench $HO^\bullet$ radicals, the observed effect not only further supports the noninvolvement of $HO^\bullet$ in DT formation but also suggests that $HO^\bullet$ is responsible for the oxidative side reactions that decrease the yield of dityrosine.

Substantial work on the chemistry of metal-catalyzed oxidative coupling of phenols (e.g., ref *34*) has revealed that reactions proceed through the initial formation of metal phenolate complexes. In our experiments in the absence of added ligands, the addition of Cu(II) to the pH 7.4 buffer resulted in immediate precipitation unless AT was also present, strongly suggesting the formation of soluble Cu(II)−tyrosinate complexes which lead to product DADT under the influence of H_2O_2.

DISCUSSION

Cu Induces SDS-Resistant Aβ Oligomerization. Aβ binds Cu with high affinity via histidine (*6*, *13*, *14*) and tyrosine (*10*) residues (*1*, *2*, *22*) and produces H_2O_2 by catalyzing the reduction of Cu(II) or Fe(III) (*3*, *4*). We recently showed that Cu oxidation conditions promote the modification of both histidine and tyrosine residues (*21*). We have now identified one of these oxidation products as dityrosine (Figures 2−5), a cross-link that may partially explain the Cu-induced SDS-resistant oligomerization of Aβ detected on PAGE (Figures 1 and 4 and Table 1). We propose that the generation of H_2O_2 by Aβ, and its interaction with Cu coordinated to tyrosine and histidine residues, damages these residues at least in part through reactions that lead to covalent cross-linking. This leads to the formation of cross-linked oligomers on PAGE (Figures 1, 3, and 4), a classical characteristic of the Aβ amyloid extracted from AD brain (*6*).

We have found that oxidation of Aβ species under these conditions is dependent upon the binding and reduction of Cu(II) by Aβ (*3*, *4*) and the generation of H_2O_2 from the Aβ−Cu(I) complex [regenerating the Aβ−Cu(II) complex], since H_2O_2 individually does not induce Aβ oligomerization (results not shown) or amino acid modification (*21*). Al-

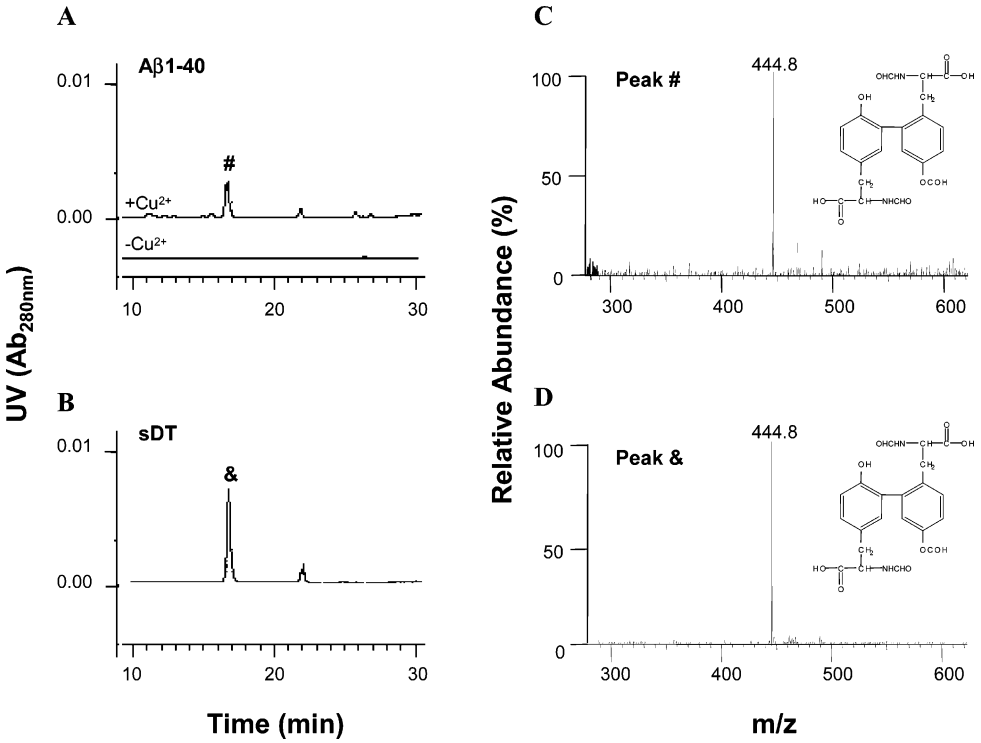

FIGURE 5: Detection of a dityrosine cross-link in Cu(II)-oxidized Aβ1−40 by HPLC and ESI-MS. (A) HPLC profile of Aβ1−40 either untreated [without Cu(II)] or treated [with Cu(II)] with $CuSO_4$ following acid hydrolysis and formyl derivatization. (B) HPLC profile of the synthetic dityrosine standard following formyl derivatization. (C) ESI-MS spectrum of the main peak (#) identified by HPLC in the Aβ1−40/Cu(II) sample (A). (D) ESI-MS spectrum of the main peak (&) identified by HPLC in the dityrosine standard sample (B). Dityrosine was detected as the *N*,*N*′,*O*-triformyldityrosine derivative (insets of panels C and D) at *m*/*z* 444.8 ($[M + H]^+$).

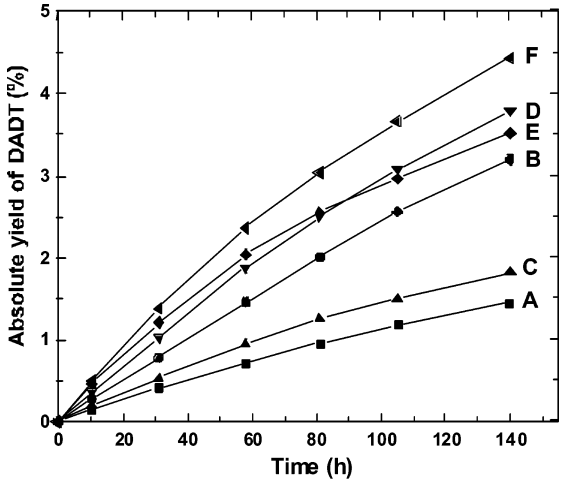

FIGURE 6: Time-dependent formation of *N*,*N*′-diacetyldi-L-tyrosine (DADT) in the H_2O_2 (5 mM)-mediated oxidation of *N*-acetyl-L-tyrosine (AT, 1 mM) catalyzed by Cu(II) (0.02 mM) in 0.1 M phosphate buffer (pH 7.4) at 25 °C, in the absence (A, C, and E) or presence (B, D, and F) of 15 mM ethylene glycol: (A and B) no ligand, (C and D) 0.08 mM imidazole, and (E and F) 0.04 mM ethylenediamine.

though Fe accumulates in amyloid plaques of the AD brain (*35*), Fe(III) does not promote the oxidative modification of Aβ (*21*), consistent with the finding that Fe does not mediate dityrosine formation (*33*). Addition of Cu(II) to solutions containing Aβ1−40 or Aβ1−42 results in the immediate precipitation of these peptides into noncovalent aggregates (*1*, *2*). Our results indicate that the formation of the covalent oligomeric species of 8.6, 13, and 17 kDa likely occurs over time within these Aβ−Cu aggregates (Figure 1). The detection of only the dimeric (8.6 kDa) species with the dityrosine antibody however indicates that the higher oligomers represent further oxidation (and perhaps oxidative coupling) of the dityrosine units in the Aβ dimers, since antibody recognition would otherwise still be seen. Our results do not preclude the involvement of alternative oxidative tyrosine coupling products (e.g., isodityrosine and pulcherosine which are generated by metal oxidation systems), or possibly the coupling of other amino acid residues. Our fluorescence data support the presence of other, as yet unidentified, conjugates in the cross-linked Aβ species. Irrespective of the mechanism of cross-linking, the generation of covalent oligomers of Aβ in amyloid deposits would lead to increased resistance to proteolytic degradation and the stabilization of Aβ. In this respect, rat Aβ, which did not form oligomeric species, is of interest since the rat does not develop cerebral Aβ deposits with age (*32*, *36*).

Although fluorescence and immunoblot signals for Aβ1−40 and Aβ1−42 in the presence of Cu(II) were similar, in the presence of Cu(II) and H_2O_2, the fluorescent signal for Aβ1−42 was ∼70% of that of Aβ1−40 (Table 1), while the level of immunoblot detection was lower again (Figure 4). The decreased fluorescence and immunoblot signals for Aβ1−42 suggest either that dityrosine cross-linking of Aβ1−42 occurs more slowly than that of Aβ1−40 or that extensive oxidative damage to the more redox active Aβ1−42 peptide (*3*, *4*) masks antibody and fluorescent detection. The generation of dityrosine fluorescence by the Aβ1−28−Cu aggregate indicated that the C-terminus of Aβ was not essential for dityrosine formation, especially in the presence of high concentrations of H_2O_2 (Figure 2).

Physiologically Relevant Mechanisms of Dityrosine Formation. Two common biochemical pathways exist for the generation of dityrosine cross-links: metal-catalyzed oxidative and peroxidase-mediated tyrosyl radical formation. Results reported here and elsewhere (*34*) reveal a mechanism for dityrosine formation mediated by Cu involving reaction of H_2O_2 with pre-existing Cu(II)−tyrosinate complexes. This reaction must generate species that have phenoxy radical-like character, which can undergo bimolecular coupling. The H_2O_2 required for this reaction could originate from sources such as activated microglia (*11*, *37*), from impaired mitochondrial function (*38*, *39*), or from Aβ itself (*3*, *4*). Consistent with a mechanism requiring coordination of Cu(II) to the tyrosine phenol group, tyrosinate ligation to Cu(II) in amyloid β-peptides has been observed by Raman spectroscopy (*40*). Although tyrosyl radicals could theoretically be generated by diffusible $HO^{\bullet}$, the latter appears to be a less efficient mechanism for generating dityrosine (*41*).

Alternatively, since dityrosine can be formed through the action of peroxidases, it is possible that dimerization of Aβ may be induced by peptide-bound Cu(II) with peroxidase-like activity, without the need for formation of a Cu(II)−phenolate complex. The neocortex contains high levels of transition metals (*19*, *42*−*46*). In AD, the concentration of each of these metal ions is 2−5-fold elevated in the neuropil, and further elevated in amyloid plaques (*19*), and there is a 2.2-fold increase in Cu concentration in cerebrospinal fluid (*47*). Given the high affinity of Aβ for Cu (*1*, *2*), the increased concentration of Cu in AD parenchyma and in amyloid deposits itself (∼390 μM; *19*) may be a reflection of Cu binding to Aβ. It should be noted that the concentrations of both Cu and Aβ used in our studies were below that detected in the AD brain [[Aβ] > 5 μM in brain tissue, and is most likely higher in amyloid deposits (*63*)]. Importantly, unlike the case with other proteins, mildly acidic conditions greatly promote the binding of Cu(II) to Aβ and its subsequent aggregation (*1*, *2*). We have shown that under mildly acidic conditions (pH 6.6), redox active Cu effectively displaces nearly all redox inert Zn from the Aβ complex (*1*, *2*). The diseased inflammatory neurochemical milieu in AD brain is characterized by acidosis (*48*) and oxidative stress (*49*−*53*). These two factors may combine to release bound Cu from proteins generally, and therefore are likely to facilitate the inappropriate transfer of Cu to Aβ (and other proteins). This could lead to excessive Aβ aggregation (*1*) and oxidative damage within the aggregate (Figures 1−6). A role for the peroxidase-like activity of redox metal ions bound to senile plaques and neurofibrillary tangles has been suggested by recent *in situ* work (*54*). Interdiction of abnormal Cu−Aβ interactions may therefore hold therapeutic promise in future treatments for AD. Indeed, we have recently reported that administration of the hydrophobic Cu/Zn chelator clioquinol to AβPP transgenic mice reverses amyloid deposition (*55*).

Cross-linking of Aβ in amyloid deposits by enzymatic peroxidation is another mechanism by which dityrosine cross-links could form in amyloid deposits. Galeazzi et al. (*56*) have previously reported that peroxidase treatment of millimolar concentrations of Aβ in the presence of H_2O_2 generated fluorescence indicative of dityrosine. Thus, activated microglial cells in the brain parenchyma closely associated with amyloid deposits (*57*−*59*), and known to release H_2O_2 and myeloperoxidase, could lead to tyrosine cross-linkage of Aβ. Indeed, we and others have reported myeloperoxidase colocalized to both amyloid plaques (*60*, *61*) and neurofibrillary tangles (*61*) in AD-affected brains, but not in age-matched control sections. The contribution of both Cu and peroxidative mechanisms to the 5−8-fold elevation of the level of total dityrosine present in the AD brain compared to normal control tissue (*62*) remains to be determined.

ACKNOWLEDGMENT

ESI-MS was performed at the Mass Spectrometry Core Facility of the Institute of Pathology, Case Western Reserve University.

REFERENCES

1. Atwood, C. S., Moir, R. D., Huang, X., Bacarra, N. M. E., Scarpa, R. C., Romano, D. M., Hartshorn, M. A., Tanzi, R. E., and Bush, A. I. (1998) Dramatic aggregation of Alzheimer Abeta by Cu(II) is induced by conditions representing physiological acidosis, *J. Biol. Chem. 273*, 12817−12826.
2. Atwood, C. S., Scarpa, R. C., Huang, X., Moir, R. D., Jones, W. D., Fairlie, D. P., Tanzi, R. E., and Bush, A. I. (2000) Characterization of copper interactions with Alzheimer Aβ peptides: Identification of a attomolar affinity copper binding site on Aβ1−42, *J. Neurochem. 75*, 1219−1233.
3. Huang, X., Atwood, C. S., Hartshorn, M. A., Multhaup, G., Goldstein, L. E., Scarpa, R. C., Cuajungco, M. P., Gray, D. N., Lim, J., Moir, R. D., Tanzi, R. E., and Bush, A. I. (1999) The Aβ peptide of Alzheimer's disease directly produces hydrogen peroxide through metal ion reduction, *Biochemistry 38*, 7609−7616.
4. Huang, X., Cuajungco, M. P., Atwood, C. S., Hartshorn, M. A., Tyndall, J., Hanson, G. R., Stokes, K. C., Multhaup, G., Goldstein, L. E., Scarpa, R. C., Saunders, A. J., Lim, J., Moir, R. D., Glabe, C., Bowden, E. F., Masters, C. L., Fairlie, D. P., Tanzi, R. E., and Bush, A. I. (1999) Alzheimer Aβ interaction with Cu(II) induces neurotoxicity, radicalization, metal reduction and hydrogen peroxide formation, *J. Biol. Chem. 274*, 37111−37116.
5. Glenner, G. G., and Wong, C. W. (1984) Alzheimer's disease: initial report of the purification and characterization of a novel cerebrovascular amyloid protein, *Biochem. Biophys. Res. Commun. 120*, 885−890.
6. Masters, C. L., Simms, G., Weinman, N. A., Multhaup, G., McDonald, B. L., and Beyreuther, K. (1985) Amyloid plaque core protein in Alzheimer disease and Down syndrome, *Proc. Natl. Acad. Sci. U.S.A. 82*, 4245−4249.
7. Haass, C., Schlossmacher, M. G., Hung, A. Y., Vigo-Pelfrey, C., Mellon, A., Ostaszewski, B. L., Lieberburg, I., Koo, E. H., Schenk, D., Teplow, D. B., et al. (1992) Amyloid beta-peptide is produced by cultured cells during normal metabolism, *Nature 359*, 322−325.
8. Seubert, P., Vigo-Pelfrey, C., Esch, F., Lee, M., Dovey, H., Davis, D., Sinha, S., Schlossmacher, M., Whaley, J., Swindlehurst, C., et al. (1992) Isolation and quantification of soluble Alzheimer's beta-peptide from biological fluids, *Nature 359*, 325−327.
9. Shoji, M., Golde, T. E., Ghiso, J., Cheung, T. T., Estus, S., Shaffer, L. M., Cai, X.-D., McKay, D. M., Tintner, R., Frangione, B., and Younkin, S. G. (1992) Production of the Alzheimer amyloid beta protein by normal proteolytic processing, *Science 258*, 126−129.
10. Kuo, Y. M., Emmerling, M. R., Vigo-Pelfrey, C., Kasunic, T. C., Kirkpatrick, J. B., Murdoch, G. H., Ball, M. J., and Roher, A. E. (1996) Water-soluble Abeta (N-40, N-42) oligomers in normal and Alzheimer disease brains, *J. Biol. Chem. 271*, 4077−4081.
11. Roher, A. E., Chaney, M. O., Kuo, Y. M., Webster, S. D., Stine, W. B., Haverkamp, L. J., Woods, A. S., Cotter, R. J., Tuohy, J. M., Krafft, G. A., Bonnell, B. S., and Emmerling, M. R. (1996) Morphology and toxicity of Abeta-(1−42) dimer derived from neuritic and vascular amyloid deposits of Alzheimer's disease, *J. Biol. Chem. 271*, 20631−20635.
12. Burdick, D., Soreghan, B., Kwon, M., Kosmoski, J., Knauer, M., Henschen, A., Yates, J., Cotman, C., and Glabe, C. (1992)

Assembly and aggregation properties of synthetic Alzheimer's A4/beta amyloid peptide analogs, *J. Biol. Chem. 267*, 546−554.
13. Hilbich, C., Kisters-Woike, B., Reed, J., Masters, C. L., and Beyreuther, K. (1991) Aggregation and secondary structure of synthetic amyloid beta A4 peptides of Alzheimer's disease, *J. Mol. Biol. 218*, 149−163.
14. Dyrks, T., Dyrks, E., Hartmann, T., Masters, C., and Beyreuther, K. (1992) Amyloidogenicity of beta A4 and beta A4-bearing amyloid protein precursor fragments by metal-catalyzed oxidation, *J. Biol. Chem. 267*, 18210−18217.
15. Dyrks, T., Dyrks, E., Masters, C. L., and Beyreuther, K. (1993) Amyloidogenicity of rodent and human betaA4 sequences, *FEBS Lett. 324*, 231−236.
16. Bush, A. I., Pettingell, W. H., Jr., Paradis, M. D., and Tanzi, R. E. (1994) Modulation of A beta adhesiveness and secretase site cleavage by zinc, *J. Biol. Chem. 269*, 12152−12158.
17. Bush, A. I., Pettingell, W. H., Multhaup, G., de Paradis, M., Vonsattel, J. P. G. J. F., Beyreuther, K., Masters, C. L., and Tanzi, R. E. (1994) Rapid induction of Alzheimer A beta amyloid formation by zinc, *Science 265*, 1464−1467.
18. Huang, X., Atwood, C. S., Moir, R. D., Hartshorn, M. A., Vonsattel, J.-P., Tanzi, R. E., and Bush, A. I. (1997) Zinc-induced Alzheimer's Abeta1−40 aggregation is mediated by conformational factors, *J. Biol. Chem. 272*, 26464−26470.
19. Lovell, M. A., Robertson, J. D., Teesdale, W. J., Campbell, J. L., and Markesbery, W. R. (1998) Copper, iron and zinc in Alzheimer's disease senile plaques, *J. Neurol. Sci. 158*, 47−52.
20. Dong, J., Atwood, C. S., Anderson, V. E., Siedlak, S. L., Perry, G., Smith, M. A., and Carey, P. R. (2003) Metal binding and oxidation of amyloid-β within isolated senile plaque cores: Raman microscopic evidence, *Biochemistry 42*, 2768−2773.
21. Atwood, C. S., Huang, X., Katri, A., Scarpa, R. C., Moir, R. D., Kim, Y.-S., Tanzi, R. E., Roher, A. E., and Bush, A. I. (2000) Copper catalyzed oxidation of Alzheimer Aβ, *Cell. Mol. Biol. 46*, 777−783.
22. Curtain, C. C., Ali, F., Volitakis, I., Cherny, R. A., Norton, R. S., Beyreuther, K., Barrow, C. J., Masters, C. L., Bush, A. I., and Barnham, K. J. (2001) Alzheimer's disease amyloid-beta binds copper and zinc to generate an allosterically ordered membrane-penetrating structure containing superoxide dismutase-like subunits, *J. Biol. Chem. 276*, 20466−20473.
23. Shen, H.-R., Spikes, J. D., Smith, C. J., and Kopecek, J. (2000) Photodynamic crosslinking of proteins V. Nature of the tyrosine-tyrosine bonds formed in the FMN-sensitized intermolecular crosslinking of *N*-acetyl-L-tyrosine, *J. Photochem. Photobiol., A 133*, 115−122.
24. Eickhoff, H., Jung, G., and Rieker, A. (2001) Oxidative phenol coupling: tyrosine dimers and libraries containing tyrosyl peptide dimers, *Tetrahedron 57*, 353−364.
25. Guo, Z.-W., Salamonczyk, G. M., Han, K., Machiya, K., and Sih, C. J. (1997) Enzymatic oxidative phenolic coupling, *J. Org. Chem. 62*, 6700−6701.
26. Nishiyama, S., Kim, M. H., and Yamamura, S. (1994) Syntheses of isodityrosine, dityrosine and related compounds by phenolic oxidation of tyrosine and phenylglycine derivatives using an electrochemical method, *Tetrahedron Lett. 35*, 8397−8400.
27. Kato, Y., Wu, X., Naito, M., Nomura, H., Kitamoto, N., and Osawa, T. (2000) Immunochemical detection of protein dityrosine in atherosclerotic lesion of apo-E-deficient mice using a novel monoclonal antibody, *Biochem. Biophys. Res. Commun. 275*, 11−15.
28. Vigo-Pelfrey, C., Lee, D., Keim, P., Lieberburg, I., and Schenk, D. B. (1993) Characterization of beta-amyloid peptide from human cerebrospinal fluid, *J. Neurochem. 61*, 1965−1968.
29. Kang, J., Lemaire, H. G., Unterbeck, A., Salbaum, J. M., Masters, C. L., Grzeschik, K. H., Multhaup, G., Beyreuther, K., and Muller-Hill, B. (1987) The precursor of Alzheimer's disease amyloid A4 protein resembles a cell-surface receptor, *Nature 325*, 733−736.
30. Miller, D. L., Papayannopoulos, I. A., Styles, J., Bobin, S. A., Lin, Y. Y., Biemann, K., and Iqbal, K. (1993) Peptide compositions of the cerebrovascular and senile plaque core amyloid deposits of Alzheimer's disease, *Arch. Biochem. Biophys. 301*, 41−52.
31. Roher, A. E., Lowenson, J. D., Clarke, S., Woods, A. S., Cotter, R. J., Gowing, E., and Ball, M. J. (1993) β-Amyloid-(1−42) is a major component of cerebrovascular amyloid deposits: implications for the pathology of Alzheimer disease, *Proc. Natl. Acad. Sci. U.S.A. 90*, 10836−10840.
32. Shivers, B. D., Hilbich, C., Multhaup, G., Salbaum, M., Beyreuther, K., and Seeburg, P. H. (1988) Alzheimer's disease amyloidogenic glycoprotein: expression pattern in rat brain suggests a role in cell contact, *EMBO J. 7*, 1365−1370.
33. Kato, Y., Kitamoto, N., Kawai, Y., and Osawa, T. (2001) The hydrogen peroxide/copper ion system, but not other metal-catalyzed oxidation systems, produces protein-bound dityrosine, *Free Radical Biol. Med. 31*, 624−632.
34. Kushioka, K., Tanimoto, I., and Maruyama, K. (1989) Oxidation of 2,4-di-*tert*-butylphenol by hydrogen peroxide catalyzed by bis(ethylenediamine)copper(II) complexes, *Bull. Chem. Soc. Jpn. 62*, 1147−1153.
35. Smith, M. A., Harris, P. L. R., Sayre, L. M., and Perry, G. (1997) Iron accumulation in Alzheimer disease is a source of redox-generated free radicals, *Proc. Natl. Acad. Sci. U.S.A. 94*, 9866−9868.
36. Johnstone, E. M., Chaney, M. O., Norris, F. H., Pascual, R., and Little, S. P. (1991) Conservation of the sequence of the Alzheimer's disease amyloid peptide in dog, polar bear and five other mammals by cross-species polymerase chain reaction analysis, *Brain Res. Mol. Brain Res. 10*, 299−305.
37. Giulian, D., Haverkamp, L. J., Yu, J., Karshin, W., Tom, D., Li, J., Kazanskaia, A., Kirkpatrick, J., and Roher, A. E. (1998) The HHQK domain of β-amyloid provides a structural basis for the immunopathology of Alzheimer's disease, *J. Biol. Chem. 273*, 29719−29726.
38. Shinobu, L. A., and Beal, M. F. (1997) The Role of Oxidative Processes and Metal Ions in Aging and Alzheimer's Disease, in *Metals and Oxidative Damage in Neurological Disorders* (Connor, J. R., Ed.) pp 237−275, Plenum Press, New York.
39. Hirai, K., Aliev, G., Nunomura, A., Russell, R. L., Atwood, C. S., Johnson, A. B., Kress, Y., Vinters, H. V., Tabaton, M., Cash, A., Siedlak, S. L., Jones, P. K., Petersen, R. B., Perry, G., and Smith, M. A. (2001) Mitochondrial DNA turnover is decreased in oxidatively stressed pyramidal neurons of the Alzheimer's disease brain, *J. Neurosci. 21*, 3017−3023.
40. Miura, T., Suzuki, K., Kohata, N., and Takeuchi, H. (2000) Metal binding modes of Alzheimer's amyloid β-peptide in insoluble aggregates and soluble complexes, *Biochemistry 39*, 7024−7031.
41. Higgins, T. G., Wells-Knecht, M. C., Detorie, N. A., Baynes, J. W., and Thorpe, S. R. (1993) Formation of *o*-tyrosine and dityrosine in proteins during radiolytic and metal-catalyzed oxidation, *J. Biol. Chem. 268*, 12341−12347.
42. Frederickson, C. J. (1989) Neurobiology of zinc and zinc-containing neurons, *Int. Rev. Neurobiol. 31*, 145−328.
43. Owen, C. A. (1982) Copper in the Nervous System, in *Physiological Aspects of Copper*, pp 160−191, Noyes Publications, Park Ridge, NJ.
44. Owen, C. A. (1982) Copper-Protein Binding: Copper Transport, in *Biochemical Aspects of Copper*, pp 177−186, Noyes Publications, Park Ridge, NJ.
45. Riederer, P., Sofic, E., Rausch, W. D., Schmidt, B., Reynolds, G. P., Jellinger, K., and Youdim, M. B. (1989) Transition metals, ferritin, glutathione, and ascorbic acid in parkinsonian brains, *J. Neurochem. 52*, 515−520.
46. Warren, P. J., Earl, C. J., and Thompson, H. S. (1960) The distribution of copper in human brain, *Brain 83*, 709−717.
47. Cherny, R. A., Legg, J. T., McLean, C. A., Fairlie, D. P., Huang, X., Atwood, C. S., Tanzi, R. E., Masters, C. L., and Bush, A. I. (1999) Aqueous dissolution of Alzheimer's disease Aβ amyloid deposits by biometal depletion, *J. Biol. Chem. 274*, 23223−23228.
48. Yates, C. M., Butterworth, J., Tennant, M. C., and Gordon, A. (1990) Enzyme activities in relation to pH and lactate in postmortem brain in Alzheimer-type and other dementia, *J. Neurochem. 55*, 1624−1630.
49. Martins, R. N., Harper, C. G., Stokes, G. B., and Masters, C. L. (1986) Increased cerebral glucose-6-phosphate dehydrogenase activity in Alzheimer's disease may reflect oxidative stress, *J. Neurochem. 46*, 1042−1045.
50. Smith, C. D., Carney, J. M., Starke-Reed, P. E., Oliver, C. N., Stadtman, E. R., Floyd, R. A., and Markesbery, W. R. (1991) Excess brain protein oxidation and enzyme dysfunction in normal aging and Alzheimer's disease, *Proc. Natl. Acad. Sci. U.S.A. 88*, 10540−10543.
51. Smith, M. A., Richey, P. L., Taneda, S., Kutty, R. K., Sayre, L. M., Monnier, V. M., and Perry, G. (1994) Advanced Maillard reaction end products, free radicals, and protein oxidation in Alzheimer's disease, *Ann. N.Y. Acad. Sci. 738*, 447−454.

52. Smith, M. A., Taneda, S., Richey, P. L., Miyata, S., Yan, S. D., Stern, D., Sayre, L. M., Monnier, V. M., and Perry, G. (1994) Advanced Maillard reaction end products are associated with Alzheimer disease pathology, *Proc. Natl. Acad. Sci. U.S.A. 91*, 5710−5714.
53. Hensley, K., Hall, N., Subramanian, R., Cole, P., Harris, M., Aksenov, M., Aksenova, M., Gabbita, S. P., Wu, J. F., Carney, J. M., Lovell, M., Markesbery, W. R., and Butterfield, D. A. (1995) Brain regional correspondence between Alzheimer's disease histopathology and biomarkers of protein oxidation, *J. Neurochem. 65*, 2146−2156.
54. Sayre, L. M., Perry, G., Harris, P. L., Liu, Y., Schubert, K. A., and Smith, M. A. (2000) In situ oxidative catalysis by neurofibrillary tangles and senile plaques in Alzheimer's disease: a central role for bound transition metals, *J. Neurochem. 74*, 270−279.
55. Cherny, R. A., Atwood, C. S., Xilinas, M. E., Gray, D. N., Jones, W. D., McLean, C. A., Barnham, K. J., Volitakis, I., Fraser, F. W., Kim, Y.-S., Huang, X., Goldstein, L. E., Moir, R. D., Lim, J. T., Beyreuther, K. T., Zheng, H., Tanzi, R. E., Masters, C. L., and Bush, A. I. (2001) Treatment of a Copper-Zinc Chelator Markedly and Rapidly Inhibits β-Amyloid Accumulation in Alzheimer Disease Transgenic Mice, *Neuron 30*, 665−676.
56. Galeazzi, L., Ronchi, P., Franceschi, C., and Giunta, S. (1999) In vitro peroxidase oxidation induces stable dimers of beta-amyloid (1−42) through dityrosine bridge formation, *Amyloid 6*, 7−13.
57. Rogers, J., Luber-Narod, J., Styren, S. D., and Civin, W. H. (1988) Expression of immune system-associated antigens by cells of the human central nervous system: relationship to the pathology of Alzheimer's disease, *Neurobiol. Aging 9*, 339−349.
58. McGeer, P. L., Akiyama, H., Itagaki, S., and McGeer, E. G. (1989) Activation of the classical complement pathway in brain tissue of Alzheimer patients, *Neurosci. Lett. 107*, 341−346.
59. Styren, S. D., Civin, W. H., and Rogers, J. (1990) Molecular, cellular, and pathologic characterization of HLA-DR immunoreactivity in normal elderly and Alzheimer's disease brain, *Exp. Neurol. 10*, 3−104.
60. Reynolds, W. F., Rhees, J., Maciejewski, D., Paladino, T., Sieburg, H., Maki, R. A., and Masliah, E. (1999) Myeloperoxidase polymorphism is associated with gender specific risk for Alzheimer's disease, *Exp. Neurol. 155*, 31−41.
61. Atwood, C. S., Huang, X., Moir, R. D., Smith, M. A., Tanzi, R. E., Roher, A. E., Bush, A. I., and Perry, G. (2001) Neuroinflammatory Responses in the Alzheimer's Disease Brain Promote the Oxidative Post-translational Modification of Amyloid Deposits, in *Alzheimer's Disease: Advances in Etiology, Pathogenesis and Therapeutics* (Iqbal, K., Sisodia, S. S., and Winblad, B., Eds.) pp 341−361, John Wiley & Sons, London.
62. Hensley, K., Maidt, M. L., Yu, Z., Sang, H., Markesbery, W. R., and Floyd, R. A. (1998) Electrochemical analysis of protein nitrotyrosine and dityrosine in the Alzheimer brain indicates region-specific accumulation, *J. Neurosci. 18*, 8126−8132.
63. Basun, H., Forssell, L. G., Wetterberg, L., and Winblad, B. (1991) Metals and trace elements in plasma and cerebrospinal fluid in normal aging and Alzheimer's disease, *J. Neural Transm. 3*, 231−258.

BI0358824